Inverted pyramidally-textured PDMS antireflective foils for perovskite/silicon tandem solar cells with flat top cell

Hou, Fuhua; Han, Can; Isabella, Olindo; Yan, Lingling; Shi, Biao; Chen, Junfan ; An, Sichong; Zeman, Miro; More Authors

DOI
10.1016/j.nanoen.2018.11.018

Publication date
2019

Document Version
Accepted author manuscript

Published in
Nano Energy

Supporting Information

Inverted Pyramidally-Textured PDMS Antireflective Foils for Perovskite/Silicon Tandem Solar Cells with Flat Top Cell

Fuhua Hou† [a, b, c], Can Han† [a, b, c, d], Olindo Isabella [d], Lingling Yan [a, b, c], Biao Shi [a, b, c], Junfan Chen [a, b, c], Shichong An [a, b, c], Zhongxin Zhou [a, b, c], Wei Huang [a, b, c], Huizhi Ren [a, b, c], Qian Huang [a, b, c], Guofu Hou [a, b, c], Xinliang Chen [a, b, c], Yuelong Li [a, b, c], Yi Ding [a, b, c], Guangcai Wang [a, b, c], Changchun Wei [a, b, c], Dekun Zhang [a, b, c], Miro Zeman [d], Ying Zhao [a, b, c] and Xiaodan Zhang [a, b, c] *

[a] *Institute of Photoelectronic Thin Film Devices and Technology of Nankai University, Tianjin 300071, P. R. China*

[b] *Key Laboratory of Photoelectronic Thin Film Devices and Technology of Tianjin, Tianjin 300071, P. R. China*

[c] *Collaborative Innovation Center of Chemical Science and Engineering (Tianjin), Tianjin 300072, P. R. China*

[d] *Photovoltaic Materials and Devices, Delft University of Technology, Mekelweg 4, 2628 CD Delft, The Netherlands*

†These authors contributed equally to this work

Corresponding Author

*E-mail address: xdzhang@nankai.edu.cn;

Experimental section

PDMS fabrication

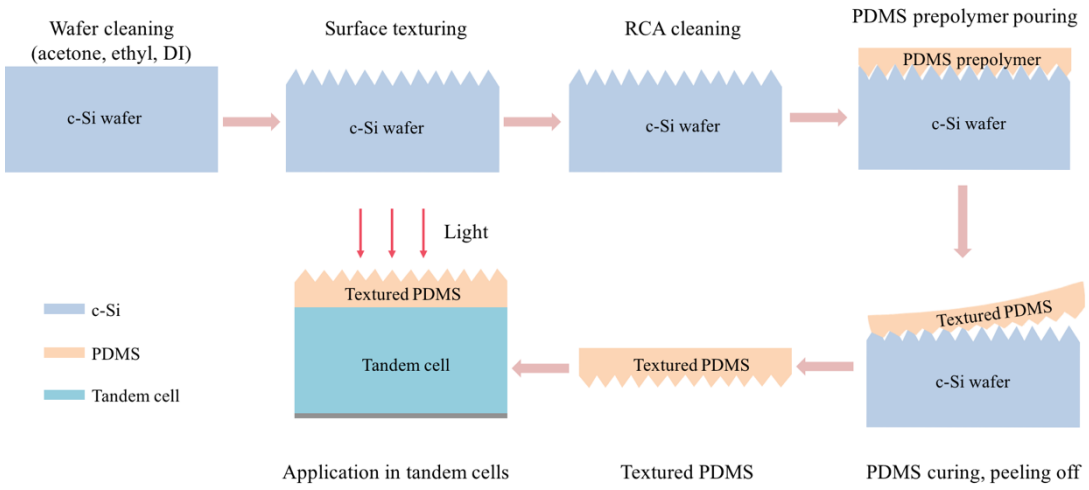

Fig. S1 Process flow of PDMS fabrication and its application in tandem solar cells

The wafers used are (100) n-type doped, obtained by FZ growth method with a resistivity of 1-10 Ω. cm. Texturization of wafers is performed using solution of NaOH diluted in isopropanol (IPA). The IPA concentration is varied to obtain three different sizes of pyramids. In all the cases, pyramid distribution includes an adequate number of sub-micronic pyramids. As no surfactants are deployed, pyramids formation follows a relatively broad distribution.

The process flow of PDMS fabrication and its application in tandem solar cell can be seen in the **Figure S1**. A 10:1 v/v ratio of PDMS and a curing agent (Sylgard 184 Silicon Elastomer from Dow Corning) was applied to a bare glass and a texture crystalline silicon (c-Si) surfaces by drop casting. The samples were then heated in a vacuum oven at 80 $^{\circ}$C for 10 h to cure and solidify the polymer. After cooling, the PDMS layer was mechanically peeled off by scraping the substrate with a razor blade. Finally, the film with pyramidal texture patterns could be laminated onto various surfaces.

Solar cell fabrication: The bottom cells used in this study were fabricated using double-sided, mirror-polished, 4-in wide, 280-µm thick, (111) oriented, n-type float zone wafers. The wafers were cleaned using the standard RCA process and the resulting oxides were removed by dipping in diluted hydrofluoric acid immediately before a-Si:H deposition. The i-a-Si:H, p-nc-SiO_x:H, and

n-nc-SiO_x:H films were prepared in three separate chambers of a RF-PECVD system to avoid cross contamination. The i-a-Si:H films were deposited with gaseous mixtures of SiH_4 and H_2. On the other hand, SiH_4, CO_2, and H_2, trimethylboron (TMB) and phosphine (PH_3) were also mixed to grow p-nc-SiOx:H and n-nc-SiOx:H films, respectively. On the front side of the wafer, 40-nm thick ITO-based tunnel recombination layers were prepared by physical vapor deposition (PVD). The back contact was formed by thermally evaporating 40-nm thick ITO and 600-nm thick Al.

The perovskite top cell was then deposited on the intermediate tunneling recombination layer with the following process flow. The substrates were cleaned with a 20-min long UV-O_3 treatment. Then, a 40-nm thick SnO_2 layer was spin coated above at a speed of 5000 rpm for 30 seconds and annealed at 150 $^{\circ}$C for 22 min. After that, the substrates were further treated by UV-O_3 for 20 min to enhance the hydrophilicity, preparatory for the subsequent deposition of perovskite precursor solutions. The perovskite precursor solution contained a mixture of CsI (0.1 M), FAI (0.9 M), PbI_2 (1.1 M), MABr (0.3 M) and $PbBr_2$ (0.3 M) in anhydrous DMF: DMSO 4:1 (v: v). Then, the perovskite film was deposited by a two-step spin coating program; first at 1000 rpm with a ramp of 200 rpm s^{-1} for 10 s; and then at 5000 rpm with a ramp of 2000 rpm s^{-1} for 50 s. During the second step, 90 µL of chlorobenzene was poured on the spinning substrate 10 s prior to the end of the program. The substrates were then transferred to hot plate for annealing at 130 °C and for 15 min in a nitrogen-filled glove box. After the perovskite annealing, the substrates were cooled down to room temperature to spin coating hole-transporting layer (HTL) on the perovskite film at 5000 rpm for 20 s. The organic HTL was prepared by dissolving spiro-OMeTAD (80 mg), TBP (28.5 µL) and LiTFSI (17.5 µL) solution (520 mg Li-TFSI in 1 mL acetonitrile) in 1 mL chlorobenzene.

Further, the 9-nm thick MoO_x was thermally evaporated on the substrate in a vacuum chamber at a base pressure around 4×10^{-5} mbar and deposition rates of 0.1 Å/s. Then the top contact was formed by 110-nm thick ITO deposited by DC magnetron sputter deposition at room temperature and without further annealing of the sample. Finally, gold electrode was thermally evaporated on the top through a shadow mask, defining a frame around the transparent cell area.

Measurements: External quantum efficiency (EQE) and reflection measurements were performed on cells before and after attachment of PDMS to study wavelength-resolved changes in absorption and reflection resulting from anti-reflection and scattering. PDMS layer was directly attached to the polished front surfaces of cells without forming an air gap. The transmission and reflection spectra were recorded with a Varian Cary 5000 UV-visible-NIR spectrophotometer with an

integrating sphere in the wavelength ranging from 300 to 1200 nm at room temperature. The morphologies of all the samples were examined using a scanning electron microscope (SEM) (QUANTA FEG 450). The PDMS replica was coated with about 30 nm of evaporated gold in SEM tests. Photocurrent density-voltage (*J-V*) curves of solar cells were measured at 25 °C in N_2-filled glovebox under the AM 1.5G (100 mW/cm^2) illumination. The monolithic tandem cell has an active area of 0.13 cm^2 defined by the overlapping area of the top and bottom sub-cell and a 0.13 cm^2 aperture was used during J-V measurement. Unless specified, bias scan was operated first from 2.0 V to -0.2 V (so-called *reverse scan*) with a voltage step of 100 mV and delay time 0.05s. Reverse curve is mainly adopted to evaluate the device performance. A solar simulator (HAL-320, ASAHI SPECTRA Co. Ltd., Japan) with compact xenon light source was used to produce the simulated AM 1.5G irradiation (100 mW/cm^2), and the calibration of the light was carried out by a detector (CS-20, ASAHI SPECTRA Co. Ltd., Japan) with silicon reference cell. The steady-state photocurrent density and efficiencies were obtained by tracking the maximum output power point, following the method described in reference. The spectral response was taken by external quantum efficiency (EQE) measurement system (QEX10, PV Measurement) in the wavelength range from 300 nm to 1200 nm with a scanning step of 10 nm. Xenon arc lamp was used as the monochromatic light excitation source and filtered by a double grating. The frequency of monochromatic light was around 80 Hz. Each individual sub-cell in the tandem must be electrically isolated to obtain an EQE spectrum. The top cell was measured by saturating the bottom cell with infrared light ($>$800 nm), whereas the bottom cell was measured by saturating the top cell with blue light (400-500 nm). No white-light bias was used during the EQE measurement.

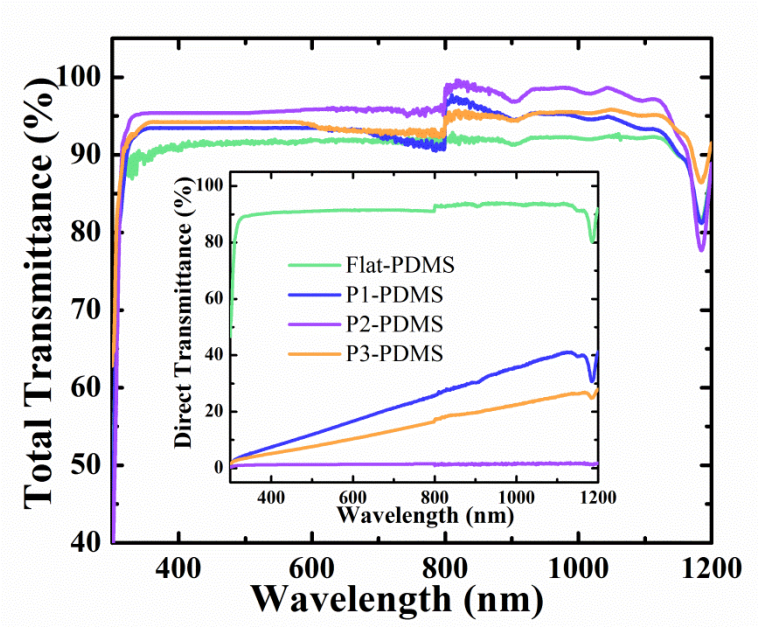

Fig. S2 Measured total and direct (inset) transmittance spectra of flat-PDMS, P1-PDMS, P2-PDMS, P3-PDMS, respectively

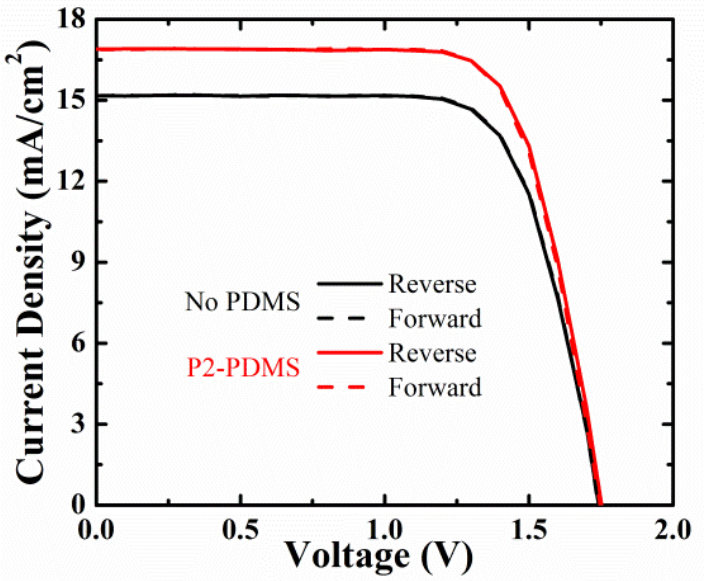

Fig. S3 Current density-voltage curves of perovskite/silicon tandem solar cell with and without the optimized P2-PDMS attached on the front surface of transparent electrode ITO.

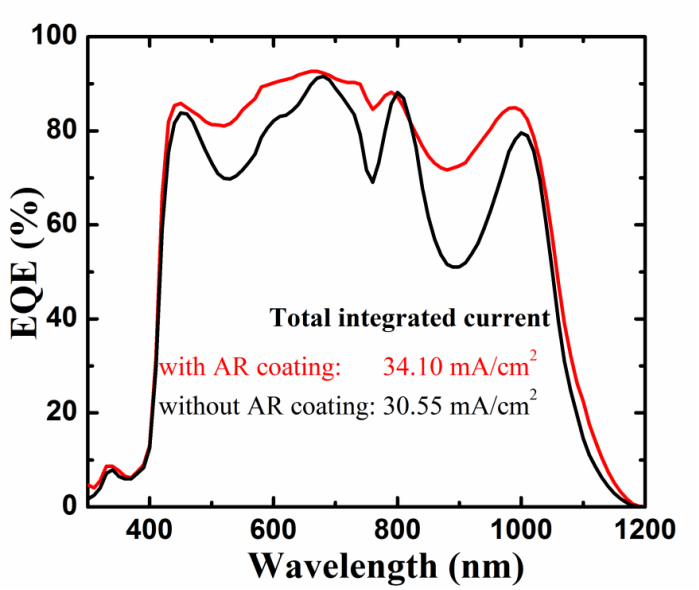

Fig. S4 The sum of the EQEs from the top perovskite and bottom silicon sub-cells.

Table S1 (a). The device parameters of tandem solar cells without PDMS attached on the front surface of transparent electrode ITO.

No PDMS	Scan direction	J_{SC} (mA/cm^2)	V_{OC} (V)	*FF*	*PCE* (%)
Device 1	Reverse	15.26	1.74	72.20	19.18
	Forward	15.25	1.74	72.26	19.17
Device 2	Reverse	15.06	1.78	73.63	19.73
	Forward	15.08	1.78	72.39	19.43
Device 3	Reverse	15.04	1.75	73.76	19.41
	Forward	15.05	1.75	73.15	19.23
Device 4	Reverse	14.93	1.78	74.69	19.85
	Forward	14.93	1.78	72.05	19.14
Device 5	Reverse	14.34	1.74	76.30	19.03
	Forward	14.37	1.74	74.96	18.74
Device 6	Reverse	15.01	1.74	72.01	18.81
	Forward	15.00	1.74	73.36	19.15

Table S1 (b). The device parameters of tandem solar cells with P2-PDMS attached on the front surface of transparent electrode ITO.

P2-PDMS	Scan direction	J_{SC} (mA/cm^2)	V_{OC} (V)	*FF*	*PCE* (%)
Device 1	Reverse	16.96	1.74	72.25	21.32
	Forward	16.95	1.74	72.28	21.32
Device 2	Reverse	16.71	1.78	73.43	21.84
	Forward	16.73	1.78	72.29	21.53
Device 3	Reverse	16.63	1.75	73.76	21.58
	Forward	16.64	1.75	73.15	21.51
Device 4	Reverse	16.52	1.78	74.69	21.99
	Forward	16.51	1.78	72.05	21.23
Device 5	Reverse	16.07	1.74	76.30	21.46
	Forward	16.19	1.74	74.96	21.12
Device 6	Reverse	16.83	1.74	72.01	21.26
	Forward	16.82	1.74	73.36	21.49

To investigate the versatility of our optimized PDMS foil, the photovoltaic performance of them on wide-bandgap perovskite solar cell (the same components of perovskite as used in the top sub-cell of tandem devices) was also tested. Fig. S5 depicts the *J-V* curves and EQE spectra of wide-bandgap perovskite solar cell with and without the optimized P2-PDMS foil attached on the front surface of glass. The device with P2-PDMS showed an obvious improvement in J_{SC} from 18.96 to 20.13 mA/cm^2 in reverse scan, and EQE over the entire wavelength range from 300 to 800 nm were increased, whereas V_{OC} and FF were nearly unchanged, as can be seen in Table S2.

The efficiency of the wide-bandgap perovskite solar cell was improved from 17.23 to 18.29% in reverse scan, mainly due to the improved J_{SC}.

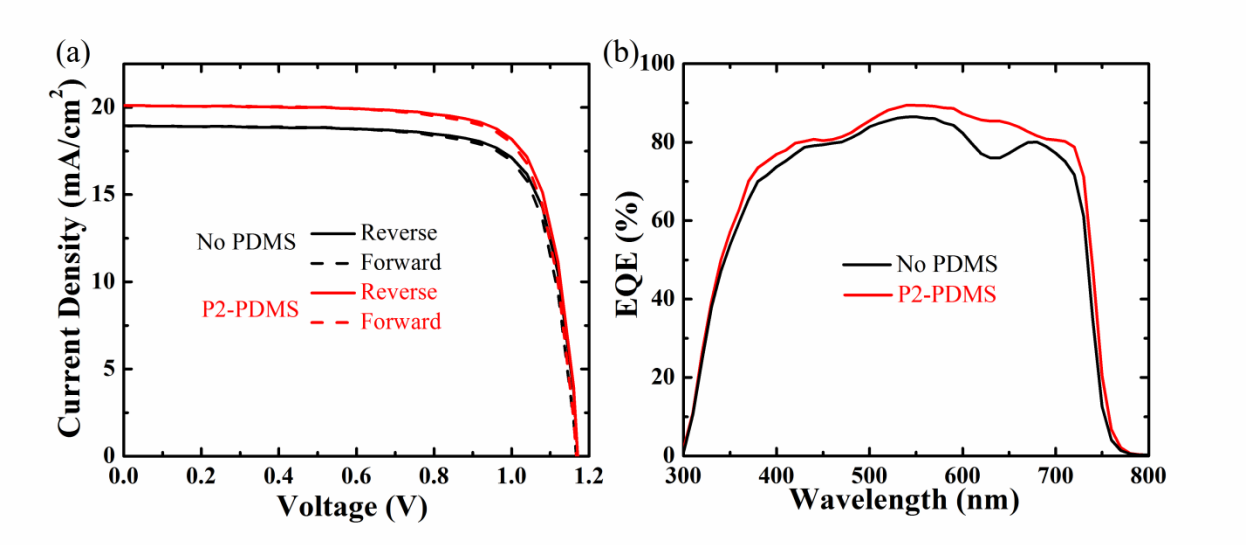

Fig. S5 (a) Current density-voltage curves and (b) external quantum efficiency (EQE) spectra of wide-bandgap perovskite solar cell with and without (no PDMS) the optimized P2-PDMS.

Table S2 Device parameters of wide-bandgap perovskite solar cell with and without (no PDMS) the optimized P2-PDMS as ARC. The data were collected under AM 1.5G one sun illumination (100 mW/cm^2).

Devices	Integrated J	Scan direction	J_{SC} (mA/cm^2)	V_{OC} (V)	*FF*	*PCE* (%)
No PDMS	18.37	Reverse	18.96	1.18	0.77	17.23
		Forward	18.95	1.18	0.76	16.70
P2-PDMS	19.46	Reverse	20.13	1.18	0.77	18.29
		Forward	20.12	1.18	0.76	18.04